Available online at www.sciencedirect.com
SCIENCE DIRECT®
Journal of Solid State Chemistry 177 (2004) 2670–2674
JOURNAL OF SOLID STATE CHEMISTRY
http://elsevier.com/locate/jssc

Multi-walled BN nanotubes synthesized by carbon-free method

Chengchun Tang,* Yoshio Bando, and Dmitri Golberg

Advanced Materials Laboratory, National Institute for Materials Science, 1-1 Namiki, Tsukuba, Ibaraki 305-0044, Japan

Received 4 March 2004; received in revised form 22 March 2004; accepted 28 March 2004

Abstract

Pure multi-walled BN nanotubes were synthesized via a carbon-free chemical vapor deposition process using boron and gallium oxide mixture as reaction precursor. Transmission electron microscopy was used to investigate their structure, morphology and defects. The wall deformation, dependent on tube diameter, was observed and explained in terms of strain relaxation of bond rotation. Opposed to carbon nanotubes, bending of BN nanotubes typically results in fracture at their concave side. Ring defect-related mechanism was proposed to interpret the fracture. The ring defects also result in the formation of a nanocone with 300° disclination. The nanocones end up with BN nanotubes exhibiting the small innermost shell ~0.4 nm in diameter.

Keywords: Boron nitride; Nanotubes; Transmission Electron Microscopy; Microstructure

1. Introduction

Although some applications have been reported in nanoelectronics, field emission, hydrogen storage, and protecting molds [1], the highest potential of BN nanotube is probably in connection with the mechanical properties, paired with high sound velocity and thermal conductivity. Various investigations [2,3] reported the axial Young's modulus of up to 1.22 TPa approaching that of carbon nanotubes (1.3–1.8 TPa) [4]. The practical engineering application needs further understanding of the elastic response and failure resistance associated with defects in BN nanotubes. Therefore, detailed experimental investigation on BN nanotube defects has been strongly desired.

The study of pure BN nanotubes has been hindered by carbon contamination when synthesizing BN nanotubes using precursors containing carbon, because carbon is the first solid phase to appear upon cooling the vapors containing boron, nitrogen, and carbon [5]. Therefore, except for few methods [6,7], the low-quality (especially from carbon contamination) BN nanotubes usually have led to the difficult characterization of their defects. Recently, we synthesized pure BN nanotubes via CVD method using a novel precursor mixture of B_2O_2 and Mg vapors [8]. The only possible contamination source, Mg, was evaporated and transported far from the reaction area. Therefore, although the formation mechanism of nanotubes warrants further investigations, the synthesized product exhibits a considerably high purity with respect to carbon contamination, making reliable the thorough defect structure analysis.

In this work, BN nanotubes were synthesized by using another reaction precursor, the mixture of boron and gallium oxide. Due to low vapor pressure of metal gallium, gallium droplet can exist at the reaction area and behaves as a catalyst of one-dimensional growth. The structure and morphology of BN nanotubes are reported and discussed in this paper.

2. Experimental

The synthetic apparatus and details were reported elsewhere [9]. In brief, an RF induction furnace was used for the synthesis. The reaction mixture of boron and gallium oxide with the molar ratio of 6:1 was thoroughly mixed and then put into an evaporation area with the temperature 1550°C to form the B_2O_2 vapor and gallium, which were transported to deposited area of

*Corresponding author.
E-mail address: tang.chengchun@nims.go.jp (C. Tang).

0022-4596/$ - see front matter © 2004 Elsevier Inc. All rights reserved.
doi:10.1016/j.jssc.2004.03.044

1100°C with an ammonia flowing and began the growth of BN nanotubes. The liquid gallium can be regarded as a vapor–liquid–solid catalyst. Structural analyses were carried out by means of high-resolution transmission electron microscopy (TEM, JEM-3000F, JEOL) operating at 300 kV.

3. Results and discussion

Fig. 1 shows a high-resolution TEM image of a multi-walled BN nanotube with 27 nm in diameter. Selected-area electron diffraction (SAED) pattern shown in the inset displays a nearly zigzag atomic arrangement, where the [10−10] direction is nearly parallel to the tube axis. Enlarged TEM images of the wall and core areas clearly exhibit a hexagonal stacking order, and fully prove the zigzag arrangement: the characteristic ~0.22 nm dot separation for the wall fringes corresponding to the (10−10) spacing in BN is visible.

The wall deformation induced by strain relaxation of bond rotation could be verified through the observation of the morphology of the tube wall (top right inset). There is rare deformation at the (010) plane normal to the tube axis; whereas a great deal of deformations is observed along the wall. The result shows that BN nanotubes are stiff along the axis, while the interplanar deformation exhibits relatively "flexibility" due to weak van der Waals forces between adjacent layers. This partly destroys the cylindrical symmetry of a nanotube.

It is also worth noting from the image that the shorter the diameter of the shell, the stronger the deformation degree. With decrease in diameter, the curvature penalty of distortion becomes more severe as the bond angles deviate far below the ideal sp^2 configuration. If considering the energy increase due to the introduction of the sp^3 character bonding for constructing a nanotube, the energy per unit length of the nanotubes is simply calculated by $E_{\text{tube}} = \pi\kappa/R$, where κ is curvature modulus, and R is tube diameter [10]. Our observation is in an agreement with the mechanism of strain relaxation strongly depending on tube diameter.

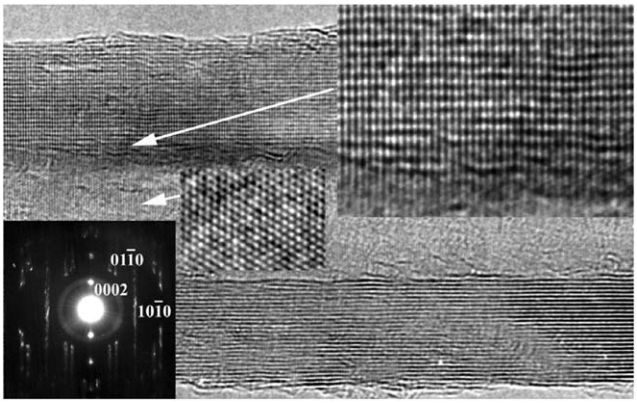

Fig. 1. High-resolution image of a multi-walled BN nanotube. Enlarged wall and core areas, and SAED patterns are shown in the inset, respectively.

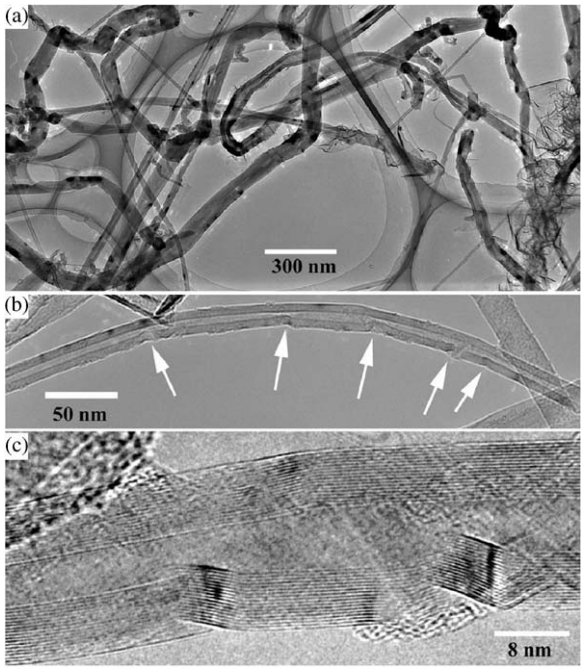

Fig. 2. Bent morphology of BN nanotubes: (a) nanotubes with large diameter show asymmetric structure at the opposite sides, the bending angles approach 90° or 39°; (b) low-magnification TEM image of a bent BN nanotube, the arrows point to the fracture points; (c) High-resolution TEM image showing the outward bucklings at both sides and fracture at the compressed side.

Another interesting defect originates from the bending of BN nanotubes. The synthesized BN nanotubular product includes various bent morphologies with diameter larger than 60 nm. The most commonly observed bending angles are approaching 40° and 90°, as shown in Fig. 2a. Moreover, most large-diameter BN nanotubes display the asymmetric structure at the opposite sides. This type of defect has been reported for thick BN nanotubes synthesized by arc-discharge of ZrB_2 electrodes, which was attributed to the pentagon–heptagon pairs and/or polyhedral cross-sections of BN nanotubes [11]. Even so, the existence of the fixed bending angles allows us to suggest that the hollow polyhedral one-dimensional BN structure is the preferential morphology for the large-diameter case, if considering that the presence of odd-member rings becomes more and more unfavorable with increase in shell diameters, since line defects composing of B–B or N–N bonds between ring-defects become longer [12].

However, for the BN nanotubes with diameter smaller than 30 nm, only the bending such as localized kinks and continuous radial deformations has been observed. Fig. 2b shows a typical continuous nanotube bending. The

bending occurs over a length of several hundred nanometers and generates a 45° bending angle. The bending occurs through a series of discontinuous local bucklings, mainly in compressed areas. High-resolution TEM image clearly exhibits the buckling morphology (Fig. 2c). It can be seen that the two sides of the bent nanotubes display similar outward buckling with respect to the tube axis, and the inner diameter of the tube continuously changes. We also noted the different curvatures for the two bent sides: the degree of the curvature $1/R$ at the concave side of the tube is obviously larger that at the convex side. The buckling is local and spreads over only about 100 nm distance. In order to preserve the cylindrical structure, a fracture is required at the concave side of the tube.

The compression and its associated buckling instability have been observed for multi-walled carbon nanotubes [13]. Therein, a stress on the concave side of the tube results in buckling, which extends into the tube until the effect of the stress on the tube is minimized. The buckling effect on the convex side is to stretch the graphene layer, while the effect is relaxed by shortening the layer length on the concave side. Therefore, an inward buckling occurs at the stress point. The possible explanation was also proposed based on the curvature effect rather than defect-related mechanism. However, the presently observed phenomena, such as fracture of BN tube on the concave side and the outward buckling at both sides, are considerably different from carbon nanotubes. Therefore, the defect-related mechanism was introduced for explaining this bending with fracture in the present case.

The tube bent morphology with fracture structure could be frequently observed in the TEM samples prepared with or without using the ultrasonic dispersion technique. The bending, thus, does not originate from the stress effect. Moreover, the maximum buckling area at the convex side, where the radius of curvature is largest, does not correspond to the fracture points at the concave side (Fig. 2c). Furthermore, the bucklings at both sides are nearly symmetrical except for the different degrees of curvature. The results imply the key role of defects for the fracture during BN nanotubes growth.

Single kink structure has been observed by Golberg et al. for a double-walled BN nanotube synthesized via oxide-promoted carbon nanotube-confined reaction method [14]. The measured kink angle of 31° was in a good agreement with the theoretically predicting angle for a pentagon–heptagon pair defect, despite the fact that the odd-ring defects are energetically unfavorable. However, as mentioned above, the larger the diameter of the tube shell, the less stable the odd-ring defects. Although the present bending of BN nanotubes with about 20 nm in diameter might be due to the odd-ring defects, theoretical calculation indicates that local defects are less likely to be comprised exclusively of even-rings, if they are stable. The existence of unstable heptagon and/or pentagon rings results in the local kink structure for the large-diameter BN shell, or the fracture structure.

A BN nanocone is another interesting object for the investigation of the ring defects. Nanocone structure can be obtained through the geometrical operation, where a sector of angle (disclination angle) is removed from a flat BN sheet, and the two cut sides of the sheet are joined together. Continuity at the junction is only satisfied if disclination angle takes certain values. Bourgeois et al. [12] found that a 240° disclination is the smallest cone geometry ensuring the presence of even-member ring defects only, while the construction of a nanocone with 300° disclination has to induce the line defect containing B–B bonds. Surprisingly, we have not observed any single nanocone-like nanotubes during TEM investigations, although some tubes with gradually decreasing diameters at their tips were frequently observed. Fig. 3a shows a "conical" BN nanotube. High-resolution TEM image showing in Fig. 3b clearly displays that the type of nanotube is not of the so-called nanocone-like structure. The diameter decrease is obtained only through a series of discontinuous dislocations near the edge of tube. The tube end still exhibits the flat tip with the characteristic zigzag atomic arrangement.

In fact, the nanocone structures we frequently observed exist as the fragments of BN nanotubes. Fig. 4a shows the typical morphology of a straight nanotube joined with a nanocone. The nanocone extends over 100 nm along the axis direction, and then transforms to a nanotube with a smaller diameter (see below). The measured apex angle is 18.9° (Fig. 4b), which is fairly close to the theoretical value of 19.2° for the apex angle of a 300° disclination [12]. The nanocones with the apex angle of 39° of 240° disclinations can be also observed.

Although the existence of 300° disclinations confirms the presence of even-ring defects, the TEM morphology

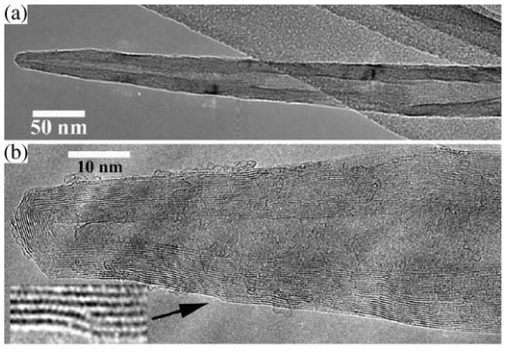

Fig. 3. (a) A conical tip of a BN nanotube and (b) its high-resolution TEM images. The gradually decreasing diameter is attributed to the edge dislocation, as shown in the inset of (b).

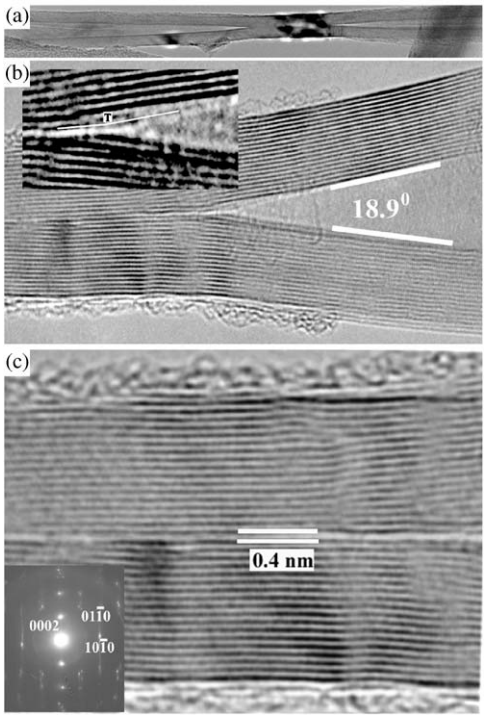

Fig. 4. Morphology changing from BN nanotube to nanocone resulting in the smallest diameter BN nanotube growth. (a) Low-magnification TEM image shows the morphology change along the axis; (b) high-magnification TEM image shows a nanocone with 300° disclination angle, the inset depicts the enlarged nanocone, and symbol "T" indicates the transition point from the nanocone to the nanotube; (c) the smallest diameter (0.4 nm) could be observed, the SAED pattern shown in the inset indicates the nanotubes with zigzag arrangements.

displays that the nanocone-like structure is not a stable energy configuration in this case. It is due to the fact that the observed nanocone does not terminate at its apex, if present, which should be a pentagon ring defect. Consequently, the growth of the nanocone stops close to the apex, and transforms to the growth of a nanotube with h-BN-like three-dimensional ordering. The transition point from nanocone to nanotube could first take place for the innermost layer of the nanocone and then expires over the whole cone via the interplanar interactions, and this finally results in the inherited nanotube growth. Enlargement of the transition area (Fig. 4b, inset) shows the morphology discussed above.

A direct consequence of this transformation of nanotube–nanocone–nanotube is the occurrence of the BN innermost nanotube with the smallest diameter. Fig. 4c displays the enlargement of this nanotube, existing at the nanocone termination (Fig. 4a). The nanotube-like morphology was verified by the experimental fact that the diameter does not vary when the sample was continuously tilted under TEM observations, and by the corresponding SAED patterns (inset, Fig. 4c). The pattern shows the similar feature of three-dimensional ordering in the plane normal to the incident beam, as that for the nanotubes with larger diameter (Fig. 1). The 18-shell BN nanotube has an average diameter for the innermost shell of approxiamtly 0.4 nm, which is variable in some areas due to the innermost shell deformation mentioned above. The average diameter of the shell corresponds to that of a $(BN)_{10}$ molecule.

The smallest multi-walled carbon nanotubes with the innermost shells of 0.4 nm diameter have been discovered. It was proposed that the nanotubes grow from a half of the C_{20} dodecahedron and a pentagon-ring defect exists at the tip [15]. Considering that the 300° disclination terminates at cone apex with the same pentagon defect, the smallest BN nanotubes described here could be considered to grow from the nanocone tip-ends. In fact, our extensive TEM observations indicate that the BN nanotubes with 0.4-nm diameter have to have a junction with a nanocone. The absence of isolate nanotubes implies that they are less stable during the growth.

In summary, the presence and the lower stability of odd-ring defects, in particular pentagons, could be used to explain the forming defects in the tube wall of pure BN nanotubes. These defects include the bending and fracture of the BN nanotubes, the nanocones with the 300° disclination angle and their ending tips, smallest BN nanotubes with the innermost shell of 0.4-nm diameter. In addition, the wall deformation dependent on tube diameter was also found and suggests the difficulty in preparing BN nanotubes with small diameters.

Acknowledgments

The authors thank Dr. F.F. Xu, and K. Kurashima for helpful discussion in TEM characterization, and Dr. T. Sato, and Dr. Y. Uemura for the support of this research.

References

[1] K. Suenaga, C. Colliex, N. Demoncy, A. Loiseau, H. Pascard, F. Willaime, Science 278 (1997) 653.
[2] N.G. Chopra, A. Zettl, Solid State Commun. 105 (1998) 297.
[3] E. Hernandez, C. Goze, P. Bernier, A. Rubio, Phys. Rev. Lett. 80 (1998) 4502.
[4] M.M.J. Treacy, T.W. Ebbesen, J.M. Gibson, Nature 381 (1996) 678.
[5] K. Suenaga, F. Willaime, A. Loiseau, C. Colliex, Appl. Phys. A 68 (1999) 301.
[6] K.P. Loh, M. Lin, M. Yeadon, C. Boothroyd, Z. Hu, Chem. Phys. Lett. 387 (2004) 40.
[7] J. Cumings, A. Zettl, Chem. Phys. Lett. 316 (2000) 211.
[8] C. Tang, Y. Bando, T. Sato, K. Kurashima, Chem. Commun. 12 (2002) 1290.
[9] C.C. Tang, Y. Bando, T. Sato, Appl. Phys. A 75 (2002) 681.

[10] R.S. Ruoff, J. Tersoff, D.C. Lorents, S. Subramoney, B. Chan, Nature 364 (1993) 514.
[11] Y. Saito, M. Maida, T. Matsumoto, Jpn. J. Appl. Phys. 38 (1999) 159.
[12] L. Bourgeois, Y. Bando, W.Q. Han, T. Sato, Phys. Rev. B 61 (2000) 7686.
[13] J.F. Despres, E. Daguerre, K. Lafdi, Carbon 33 (1995) 87.
[14] D. Golberg, Y. Bando, L. Bourgeois, K. Kurashima, T. Sato, Appl. Phys. Lett. 77 (2000) 1979.
[15] L.C. Qin, X. Zhao, K. Hirahara, Y. Miyamoto, Y. Ando, S. Iijima, Nature 408 (2000) 50.